Journal of Biomedical Optics

SPIEDigitalLibrary.org/jbo

New method for detection of gastric cancer by hyperspectral imaging: a pilot study

Shu Kiyotoki
Jun Nishikawa
Takeshi Okamoto
Kouichi Hamabe
Mari Saito
Atsushi Goto
Yusuke Fujita
Yoshihiko Hamamoto
Yusuke Takeuchi
Shin Satori
Isao Sakaida

SPIE

New method for detection of gastric cancer by hyperspectral imaging: a pilot study

Shu Kiyotoki,[a] Jun Nishikawa,[a] Takeshi Okamoto,[a] Kouichi Hamabe,[a] Mari Saito,[a] Atsushi Goto,[a] Yusuke Fujita,[b] Yoshihiko Hamamoto,[b] Yusuke Takeuchi,[c] Shin Satori,[c] and Isao Sakaida[a]
[a]Yamaguchi University Graduate School of Medicine, Department of Gastroenterology and Hepatology, Yamaguchi, Japan
[b]Yamaguchi University Graduate School of Medicine, Department of Biomolecular Engineering, Yamaguchi, Japan
[c]Hokkaido Institute of Technology, Sapporo, Japan

Abstract. We developed a new, easy, and objective method to detect gastric cancer using hyperspectral imaging (HSI) technology combining spectroscopy and imaging A total of 16 gastroduodenal tumors removed by endoscopic resection or surgery from 14 patients at Yamaguchi University Hospital, Japan, were recorded using a hyperspectral camera (HSC) equipped with HSI technology Corrected spectral reflectance was obtained from 10 samples of normal mucosa and 10 samples of tumors for each case The 16 cases were divided into eight training cases (160 training samples) and eight test cases (160 test samples) We established a diagnostic algorithm with training samples and evaluated it with test samples Diagnostic capability of the algorithm for each tumor was validated, and enhancement of tumors by image processing using the HSC was evaluated The diagnostic algorithm used the 726-nm wavelength, with a cutoff point established from training samples The sensitivity, specificity, and accuracy rates of the algorithm's diagnostic capability in the test samples were 78.8% (63/80), 92.5% (74/80), and 85.6% (137/160), respectively Tumors in HSC images of 13 (81.3%) cases were well enhanced by image processing Differences in spectral reflectance between tumors and normal mucosa suggested that tumors can be clearly distinguished from background mucosa with HSI technology. *© The Authors. Published by SPIE under a Creative Commons Attribution 3.0 Unported License. Distribution or reproduction of this work in whole or in part requires full attribution of the original publication, including its DOI.* [DOI: 10.1117/1.JBO.18.2.026010]

Keywords: corrected spectral reflectance; esophagogastroduodenoscopy; hyperspectral camera; hyperspectral imaging; flexible spectral imaging color enhancement; narrow-band imaging; spectral reflectance.

Paper 12644 received Sep. 27, 2012; revised manuscript received Dec. 18, 2012; accepted for publication Jan. 2, 2013; published online Feb. 6, 2013.

1 Introduction

Gastric cancer is the second most frequent cause of cancer-related death worldwide,[1] and the number of deaths due to gastric cancer is about 15% of the total cancer deaths in Japan.[2] Esophagogastroduodenoscopy (EGD) is widely used for the screening of gastric cancer in Japan;[3] however, skill is required to detect small gastric cancers by this method. Such cancers are often missed by EGD; the reported miss rate for gastric cancers is approximately 20%.[4] Although image-enhanced endoscopic technologies such as narrow-band imaging (NBI)[5] and flexible spectral imaging color enhancement (FICE)[6] have been developed, they are not sufficient to improve the detection rate of gastric cancers.

Hyperspectral imaging (HSI) represents a hybrid modality of optical diagnostics that obtains spectroscopic information and renders it in image form.[7] This technology has been used in the field of remote sensing. The HSC1700 hyperspectral camera (HSC; EBA JAPAN Co., Ltd., Tokyo, Japan) is equipped with HSI technology, and the images recorded by the HSC1700 include spectral reflectance (SR) at 72 spectral bands in the wavelength range from 400 to 800 nm, at wavelength intervals of approximately 5.6 nm. Satori et al. reported that at these intervals, it was possible to distinguish slight changes of color with a high degree of accuracy.[8]

We recorded gastroduodenal tumors removed by endoscopic resection or surgery using HSC and found a difference of SR between tumors and normal mucosa in resected specimens *ex vivo*. The goal of the present study was to develop a new method for detecting gastric cancers based on differences in SR between tumors and normal mucosa.

2 Methods

2.1 *Patients*

A total of 16 lesions from 14 patients who were treated in Yamaguchi University Hospital in Japan were examined. The clinicopathological characteristics of the lesions are shown in Table 1. In the study, 10 early gastric carcinomas and 4 gastric adenomas were endoscopically resected, and 1 advanced gastric carcinoma and 1 carcinoma of the duodenum were surgically resected. These resected specimens were used for evaluation of SR by HSC.

We obtained institutional review board approval from our university. The patients received complete information on this study before providing their consent for participation, and research was carried out in accordance with the Declaration of Helsinki.

2.2 *Characteristics of the HSC1700*

The HSC1700 can obtain SR for 72 spectral bands in the wavelength range from 400 to 800 nm in an image with a size of

Address all correspondence to: Jun Nishikawa, Yamaguchi University Graduate School of Medicine, Department of Gastroenterology and Hepatology, Yamaguchi, Japan. Tel: +81-836-22-2241; Fax: +81-836-22-2240; E-mail: junnis@yamaguchi-u.ac.jp

Table 1 Characteristics of the cases recorded by HSC.

Group	Case no.	Sex	Age (y)	Treatment method	Location	Histopathologic diagnosis	Depth	Macroscopic type	Color	Tumor size (mm)
Training	1	F	76	ER	M	Adenoma	m	Protruding	Discolored	20
	2	F	76	ER	M	Adenoma	m	Protruding	Discolored	10
	3	M	71	ER	M	Tub1	m	Protruding	Reddish	20
	4	F	79	ER	L	Pap	m	Depressed	Reddish	6
	5	M	76	ER	L	Tub1	m	Protruding	Discolored	22
	6	F	67	ER	L	Adenoma	m	Protruding	Same	12
	7	M	86	ER	M	Tub1	m	Protruding	Same	18
	8	M	84	ER	M	Tub1	m	Depressed	Reddish	10
Test	9	M	81	ER	L	Adenoma	m	Protruding	Same	10
	10	M	70	ER	L	Tub1	m	Depressed	Reddish	12
	11	M	64	ER	L	Tub1	sm	Protruding	Discolored	38
	12	M	68	ER	L	Tub1	m	Depressed	Reddish	8
	13	M	68	ER	L	Tub1	m	Depressed	Reddish	8
	14	F	65	ER	U	Tub2	m	Depressed	Reddish	28
	15	M	59	Surgery	D	Tub1	m	Protruding	Discolored	20
	16	M	78	Surgery	M	Pap	ss	Protruding	Reddish	20

Note: ER, endoscopic resection; U, upper third of the stomach; M, middle third of the stomach; L, lower third of the stomach; D, duodenum; Tub1, well-differentiated adenocarcinoma; Tub2, moderately differentiated adenocarcinoma; Pap, papillary adenocarcinoma; m, mucosa; sm, submucosa; ss, subserosa; Same, same color as normal mucosa.

640 × 480 pixels. A representative HSC image and SR data for each wavelength in tumorous and normal mucosae from Case 1 are shown in Fig. 1. The SR at all pixels in the image can be evaluated with HSC analysis software (HSD Analysiser; EBA JAPAN Co.). The obtained SR is normalized to one on the basis of white reference data.

2.3 *Recording Procedure with the HSC*

The 16 resected specimens were washed with buffered saline and as much of the mucus as possible was removed; then the specimens were pinned on blackboards and immediately recorded with the HSC. All specimens were illuminated equally using the diffused light of three 250-W halogen lamps. The distance between the HSC and the specimen was 50 cm (Fig. 2). Images of the tumors and surrounding normal mucosa could be obtained for all specimens.

2.4 *Pathological Evaluation of the Resected Specimens*

After being recorded by HSC, the resected specimens were fixed in 10% buffered formalin. We followed the 14th edition of the *Japanese Classification of Gastric Carcinoma* with regard to the handling of resected specimens.[9] The fixed specimens were sectioned at 2-mm intervals and stained with hematoxylin and eosin. The border between the tumor and normal mucosa was diagnosed by histopathological examination. All lesions were curatively resected with a sufficient margin.

2.5 *Analysis of the SRs of Tumors and Normal Mucosae*

The method of supervised learning was used to establish a diagnostic algorithm and evaluate its diagnostic capability.[10] The 16 cases were divided into eight training cases and eight test cases. The training cases were used to determine the optimal wavelength and cutoff point to discriminate between normal and tumorous mucosae. The test cases, which were independent of the training cases, were used to evaluate the diagnostic capability for tumors.

The SRs were obtained from 15 samples (pixels) of normal mucosae and 10 samples (pixels) of tumors from each case. Artifacts of electric cauterization and surgical margins were omitted from the measured samples. Because the SR varied in each case, the mean SR from five normal samples was used as a control for normalization. For each case, corrected spectral reflectance (cSR) was defined as follows:

$$\text{Corrected spectral reflectance (cSR)} = \text{SR-mean SR of 5 normal samples}$$

Then the cSRs from 10 normal mucosa samples and 10 tumor samples of each case were obtained. A flowchart of the SR analysis is shown in Fig. 3.

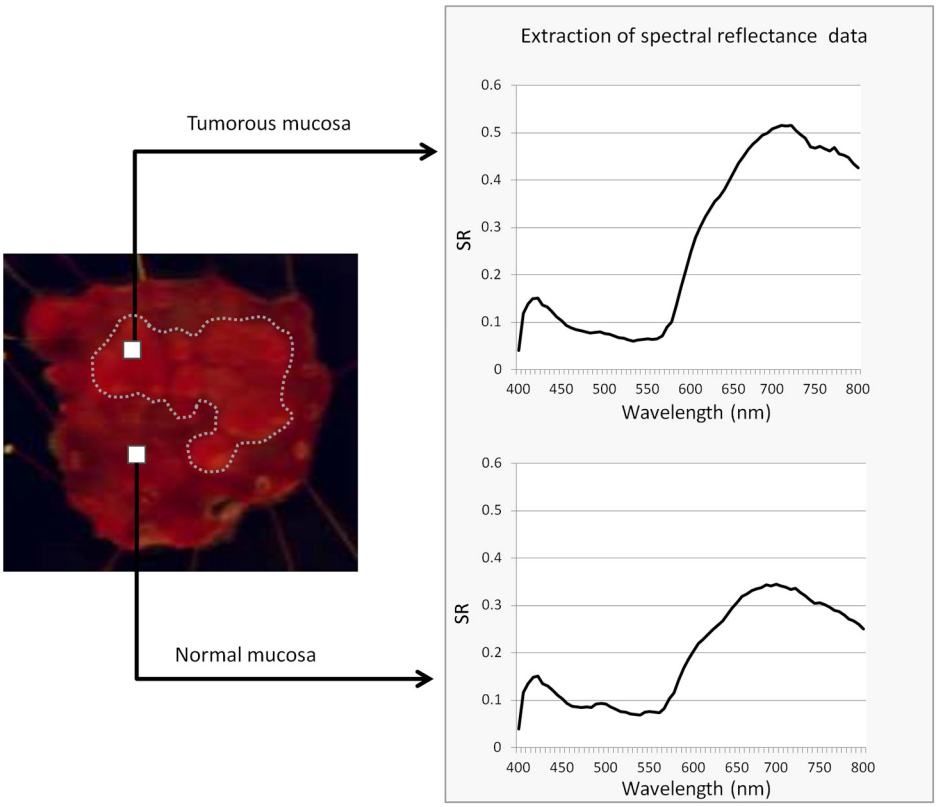

Fig. 1 Image from Case 1 obtained with the HSC and SR. Each individual pixel in the image recorded with the HSC has an SR in the wavelength range from 400 to 800 nm. By selecting any pixel, the SR of the spot can be extracted.

2.6 *Image Enhancement of Tumors by Image Processing*

By using the HSD Analysiser, we processed the images of all lesions with 20 levels of color gradation on the basis of the SR of the optimal wavelength. Each pixel of the image was displayed in blue if the SR of the pixel was low and red if it was high. The enhanced images were classified by two endoscopists (J. Nishikawa and T. Okamoto) into the following three grades: A, the entire tumor was enhanced; B, the tumor was partially enhanced; and C, the tumor was not enhanced at all. The

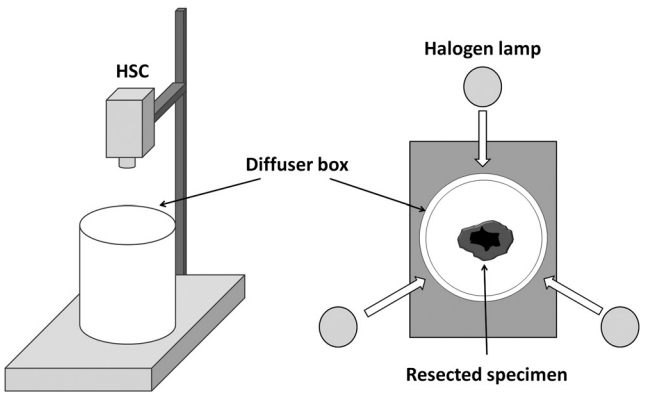

Fig. 2 Schematic of the recording procedure using the HSC. All specimens are illuminated equally using the diffused light of three 250-W halogen lamps. The distance between the HSC and the specimen is 50 cm.

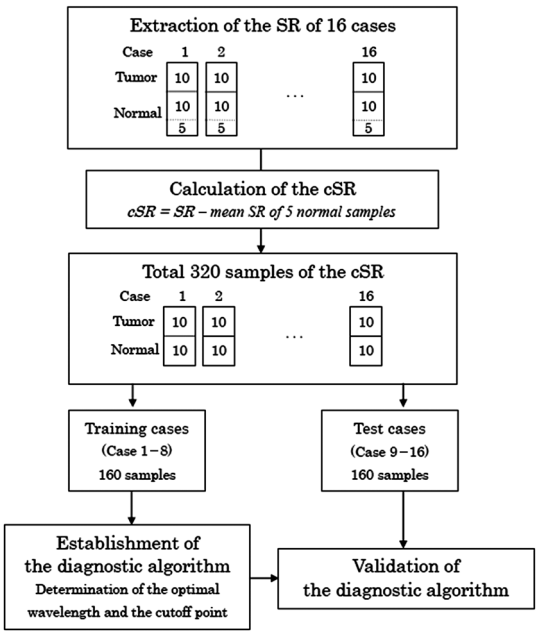

Fig. 3 Flowchart of the analysis of SR. The SR is obtained from 15 samples (pixels) of normal mucosae and 10 samples (pixels) of tumors from each case. The mean SR from 5 normal samples is used as a control for normalization, and then the cSR from 10 normal mucosa samples and 10 tumor samples of each case are obtained. The 16 cases are divided into eight training cases and eight test cases. The training cases are used to determine the optimal wavelength and cutoff point to discriminate between normal and tumorous mucosae. The test cases are used to evaluate the diagnostic capability for tumors.

cases classified as A or B were defined as "enhanced," and we examined the cases of enhancement.

3 Results

3.1 *Establishment of the Diagnostic Algorithm with Training Cases*

The mean cSR of each wavelength from the 10 tumor samples and 10 normal samples of Case 1 is shown in Fig. 4. In the range of 600 to 800 nm, the mean cSR in the tumors tended to be higher than that in normal mucosae in the training cases. Consequently, the cutoff point was set at the intermediate value between the mean cSR of 80 tumor samples and the mean cSR of 80 normal mucosal samples from the eight training cases. We hypothesized that a cSR higher than the cutoff point indicated a tumor, and a cSR lower than the cutoff point indicated normal mucosa. To determine the optimal wavelength and cutoff point, we set a cutoff point for each wavelength and compared the sensitivity, specificity, and diagnostic accuracy. The accuracy rate using the cutoff point of 726 nm was the highest for the 72 wavelengths, and its cutoff point was 0.05084. The sensitivity, specificity, and accuracy rates were 76.2% (61/80 samples), 78.8% (63/80), and 77.5% (124/160), respectively (Fig. 5).

3.2 *Validation of the Diagnostic Algorithm with Test Cases*

To evaluate the diagnostic capability using the cutoff point of the optimal wavelength (726 nm) determined in training cases, we used 160 blind samples (80 tumor samples and 80 normal mucosa samples) from the test cases, independent of the training cases. The sensitivity, specificity, and accuracy rates were 78.8% (63/80 samples), 92.5% (74/80), and 85.6% (137/160), respectively, in the test cases (Fig. 6).

3.3 *Evaluation of Images Enhanced by SR Data at 726 nm*

HSC images of the 16 cases were processed on the basis of the SR of the wavelength of 726 nm. An image from Case 1 is shown in Fig. 7. Endoscopist J. Nishikawa classified them as follows: A, 8 cases; B, 6 cases; and C, 2 cases, whereas T. Okamoto considered the classifications to be as follows: A, 3 cases; B, 11 cases; and C, 2 cases. The number of cases evaluated as enhanced (A or B) by both endoscopists was 13 (81.3%).

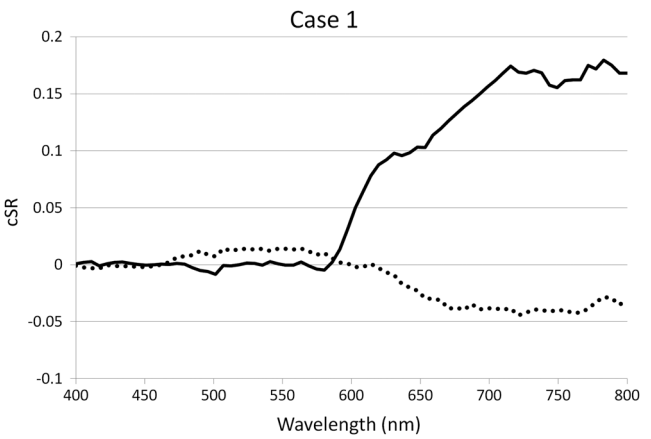

Fig. 4 Example of the cSR from the training cases. The mean cSR of the tumor and the normal mucosa from Case 1 are shown. Solid line: tumor; dashed line: normal mucosa.

4 Discussion

Previous applications of optical spectroscopy to detect gastrointestinal cancer have been attempted. Sambongi et al. measured the spectral intensities of tumors and normal mucosae of the stomach and the colon using a fiber probe through an endoscope.[11] They analyzed the SR in the range of 400 to 600 nm normalized to an SR of 640 nm, but the difference in SR between tumors and normal mucosae was not clearly identified. The usefulness of autofluorescence for cancer detection has been reported. Mayinger et al. measured the fluorescence

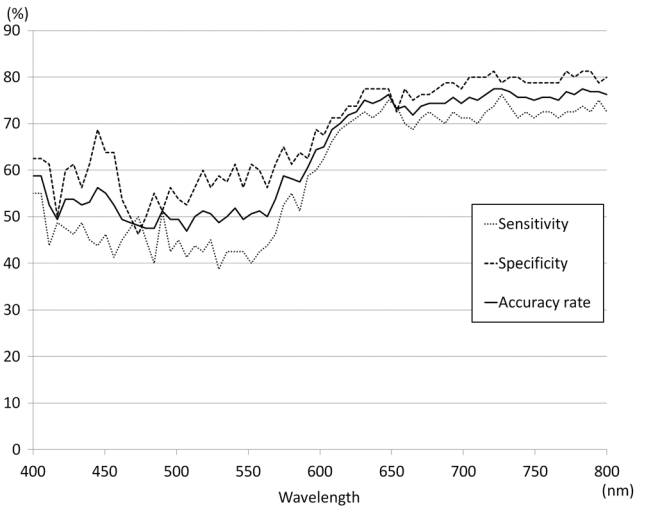

Fig. 5 Sensitivity, specificity, and diagnostic accuracy of each wavelength in the training cases. The cutoff point is set at the intermediate value between the mean cSR of 80 tumor samples and the mean cSR of 80 normal mucosal samples from the eight training cases. The accuracy rate using the cutoff point of 726 nm is the highest for the 72 wavelengths.

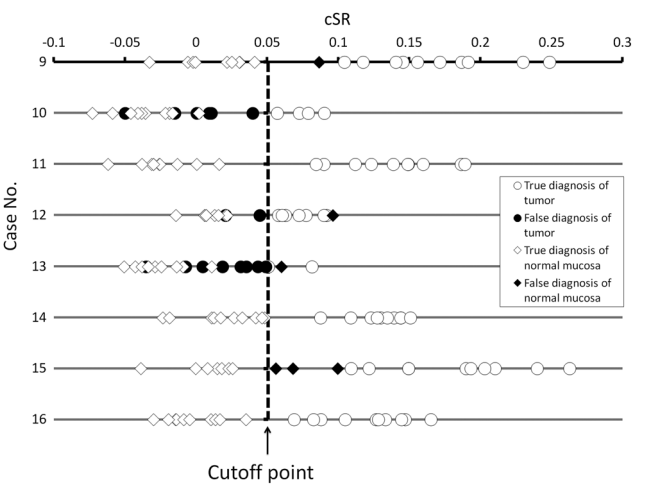

Fig. 6 Diagnostic accuracy of the cSR at the 726-nm wavelength in the test cases. Using the cutoff point (0.05084) determined for the training cases, 160 test case samples were diagnosed as tumors or normal mucosae. The sensitivity, specificity, and accuracy rates are 78.8% (63/80 samples), 92.5% (74/80), and 85.6% (137/160), respectively.

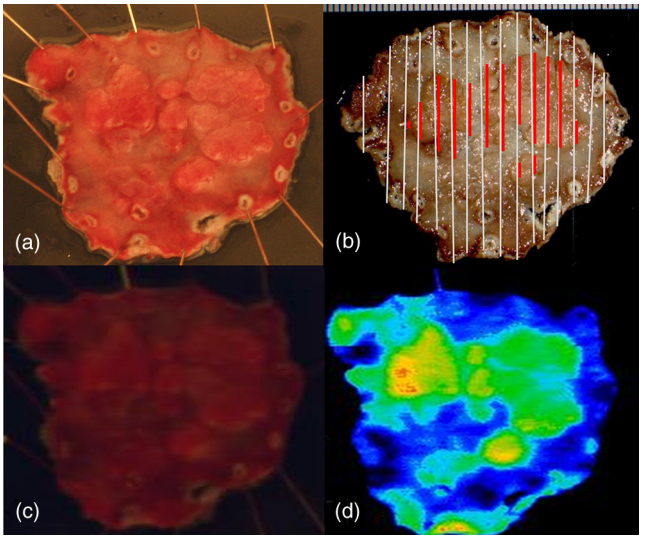

Fig. 7 Image processing on the basis of the SR at the 726-nm wavelength. A resected specimen from Case 1 is shown. (a) Digital camera image before recording with the HSC. (b) Image of the resected specimen fixed in 10% buffered formalin. The fixed specimen is sectioned at 2-mm intervals, and the tumorous areas are diagnosed by histopathological examination. We indicated the cut lines made at 2-mm intervals as white lines on the specimens and the tumorous areas compared with the histopathological results with red lines. (c) HSC image before image processing. (d) Image processed on the basis of the SR at the 726-nm wavelength by using HSD Analysiser. Each pixel of the image is displayed in blue if the SR of the pixel is low and in red if it is high. The tumor-emphasized areas and the histopathologically determined tumorous areas are almost identical.

spectra of gastric cancer by illumination with violet-blue light through a fiber probe, and a sensitivity of 84% and specificity of 87% were obtained for the diagnosis of gastric adenocarcinoma.[12] Because both systems could obtain the spectral data of only a single spot, it was impossible to evaluate the spectrum over a large area of observation. By contrast, the advantage of HSI technology is that it can obtain spectral data for each pixel in an image with a large area of observation.[7,8] This enables the comparison of spectral data between the tumor and normal mucosa and visualization of the difference by image processing.

We measured the SR of resected specimens of gastric cancers using the HSC1700; however, SR varied in each case. It is thought that SR is reflected mainly by surface color. Gastric cancers have various colors (ranging from reddish to discolored) in each patient. In addition, the color of the background mucosa also varies with gastritis and the grade of mucosal atrophy, and these changes may also provide variations in the SR. Therefore, the mean SR in normal mucosa was used as a control for normalization, making it possible to effectively reduce variation and determine the optimal wavelength and cutoff point to discriminate between normal and tumorous mucosae. The accuracy rate using the optimal wavelength of 726 nm was the highest among the 72 wavelengths examined in the training cases. The diagnostic algorithm based on the analysis of the training cases was applied to test cases and led to highly accurate diagnoses.

With regard to the clinical setting, we are considering that an endoscope and an HSC are connected to measure reflectance spectra of gastric cancer *in vivo*. When we develop such a prototype, SR of normal mucosa will be measured first, and images of cancerous areas with SR very different from the normal will be enhanced during endoscopic examination. We believe that application of HSI to endoscopic examination could decrease the incidence of missed gastric cancer.

We believe that higher specificity and fewer false negatives are preferable for cancer screening. In the present study, what resulted in a false negative was very low-grade malignant gastric cancer such as that in Case 13, which suggests that differences in SR in such cases may be small.

It is not known why the SR at 726 nm is generally higher in cancerous mucosae. We first speculated that this particular SR could be affected by the hemoglobin concentration because microvessel density correlated positively with the SR at the wavelength of 726 nm in the lesions (data not shown in this article). Oxyhemoglobin is normally the most abundant form of hemoglobin and has three peaks of absorption (418, 542, and 577 nm).[13] Image-enhanced endoscopic techniques such as NBI and FICE have mainly utilized light wavelengths of 400 to 600 nm.[5,6] These are suitable for the detection of capillary-rich tumors and observation of irregular microvessels on tumors with a magnifying endoscope.[14,15] The 726-nm wavelength of light has a tendency to be absorbed more easily by deoxyhemoglobin.[16,17] Therefore, the difference of SR at 726 nm might be associated with the deoxyhemoglobin content. We also considered other factors influencing the absorption and scattering of light. The 726-nm wavelength is near-infrared light, and it can penetrate the mucosal layer to the submucosal layer,[18] so interstitial collagen in this layer might affect the SR at 726 nm.[19]

The limitations of this study include the small sample size and the fact that all the results obtained with the HSC were from *ex vivo* SR data. It is not known if the same results would be obtained with *in vivo* data. There is a high possibility that hemoglobin density and oxygen saturation having an effect on SR are considered to change with *in vivo* and *ex vivo* tissue. Therefore, in order to determine whether the *ex vivo* results of this study can be applied *in vivo*, we are planning to measure SR of gastric cancer *in vivo*.

In conclusion, we found a difference in the SR between tumors and normal mucosae *ex vivo*, indicating that it is possible to discriminate tumors from normal mucosae with this HSI system. Thus, HSI technology can be used in a computer-aided detection system that could potentially improve the detection rate of gastric cancers.

References

1. K. D. Crew and A. I. Neugut, "Epidemiology of gastric cancer," *World J. Gastroenterol.* **12**(3), 354–362 (2006).
2. S. Hirobashi, Ed., *Cancer Statistics in Japan*, p. 12, Foundation for Promotion of Cancer Research, Tokyo (2009).
3. C. Hamashima et al., "The Japanese guidelines for gastric cancer screening," *Jpn. J. Clin. Oncol.* **38**(4), 259–267 (2008).
4. K. Aida et al., "Clinicopathological features of gastric cancer detected by endoscopy as part of annual health checkup," *J. Gastroenterol. Hepatol.* **23**(4), 632–637 (2008).
5. K. Gono et al., "Appearance of enhanced tissue features in narrow-band endoscopic imaging," *J. Biomed. Opt.* **9**(3), 568–577 (2004).
6. J. Pohl et al., "Computed virtual chromoendoscopy: a new tool for enhancing tissue surface structures," *Endoscopy* **39**(1), 80–83 (2007).
7. T. Vo-Dinh et al., "A hyperspectral imaging system for *in vivo* optical diagnostics. Hyperspectral imaging basic principles, instrumental systems, and applications of biomedical interest," *IEEE Eng. Med. Biol. Mag.* **23**(5), 40–49 (2004).
8. S. Satori et al., "Hyperspectral sensor HSC3000 for Nano-satellite 'TAIKI'," *Proc. SPIE* **7149**, 71490M (2008).

9. Japanese Gastric Cancer Association, Ed., *Japanese Classification of Gastric Carcinoma*, 14th ed., pp. 21–25, Kanehara, Tokyo (2010).
10. A. K. Jain, R. P. W. Duin, and J. Mao, "Statistical pattern recognition: a review," *IEEE Trans. Pattern Anal. Mach. Intell.* **22**(1), 4–37 (2000).
11. M. Sambongi et al., "Analysis of spectral reflectance using normalization method from endoscopic spectroscopy system," *Opt. Rev.* **9**(6), 238–243 (2002).
12. B. Mayinger et al., "Evaluation of *in vivo* endoscopic autofluorescence spectroscopy in gastric cancer," *Gastrointest. Endosc.* **59**(2), 191–198 (2004).
13. S. Prahl, "Optical absorption of hemoglobin," 15 December 1999, http://omlc.ogi.edu/spectra/hemoglobin/index.html (31 January 2012).
14. T. Nakayoshi et al., "Magnifying endoscopy combined with narrow band imaging system for early gastric cancer: correlation of vascular pattern with histopathology (including video)," *Endoscopy* **36**(12), 1080–1084 (2000).
15. K. Sumiyama et al., "Combined use of a magnifying endoscope with a narrow band imaging system and a multibending endoscope for en bloc EMR of early-stage gastric cancer," *Gastrointest. Endosc.* **60**(1), 79–84 (2004).
16. P. Taroni et al., "Time-resolved optical spectroscopy and imaging of breast," *Opto-Electron Rev.* **12**(2), 249–253 (2004).
17. W. G. Zijlstra, A. Buursma, and W. P. Meeuwsen-van der Roest, "Absorption spectra of human fetal and adult oxyhemoglobin, de-oxyhemoglobin, carboxyhemoglobin, and methemoglobin," *Clin. Chem.* **37**(9), 1633–1638 (1991).
18. A. N. Bashkatov et al., "Optical properties of human skin, subcutaneous and mucous tissues in the wavelength range from 400 to 2000 nm," *J. Phys. D: Appl. Phys.* **38**(15), 2543–2555 (2005).
19. I. Georgakoudi et al., "NAD(P)H and collagen as *in vivo* quantitative fluorescent biomarkers of epithelial precancerous changes," *Cancer Res.* **62**(3), 682–687 (2002).